

1 **Potentiality of clay raw materials from northern Morocco in ceramic industry: Tetouan and**
2 **Meknes areas**

3 *M.El Ouahabi¹, L.Daoudi², F.De Vleeschouwer^{3,4}, R. Bindler⁵, N.Fagel¹

4
5 ¹ UR Argile, Géochimie et Environnement Sédimentaires (AGEs), Département de Géologie B.18, Sart-
6 Tilman, Université de Liège, Liège, B-4000, Belgium

² Département de Géologie, Faculté des Sciences et Techniques, BP 549, Marrakech, Maroc

7 ³ Université de Toulouse; INP, UPS; EcoLab (Laboratoire Ecologie Fonctionnelle et Environnement) ;
8 ENSAT, Avenue de l'Agrobiopole, 31326 Castanet Tolosan, France

⁴ CNRS; EcoLab; 31326 Castanet Tolosan, France

9 ⁵ Department of Ecology and Environmental Sciences, Umeå University, KBC-huset, plan 5, Linnaeus
10 väg 6, Umeå, Sweden

11
12
13
14 *Corresponding author: Département de Géologie, Sart-Tilman B18, Allée du 6 Août, B-4000 Liège,
15 Belgium
16 Tel: +32. (0)4.366.2210 ; Fax: +32. (0)4.366. 2029
17 E-mail address: Meriam.ElOuahabi@doct.ulg.ac.be
18
19

20 **ABSTRACT**

21 This study aims at evaluating the potential suitability of Tetouan and Meknes (central Morocco) clay
22 material as raw materials in various ceramic applications by investigating their textural, chemical, thermal
23 and firing characteristics. Textural properties were identified by specific surface area, cation exchange
24 capacity (CEC) and bulk density (ρ_s). Chemical and thermal properties were assessed using XRF and
25 TG/DTA techniques, respectively. Firing characteristics at temperatures from 800°C to 1100°C were
26 determined by linear firing shrinkage, loss on weight and water absorption capacity.
27 The Meknes clays are characterised by medium cation exchange capacity (CEC) and specific surface area
28 (SSA) values due to their moderate smectite content. The Tetouan clays have medium to low CEC and
29 medium SSA values. The main oxides in the clayey samples are SiO₂ (35 – 54.3 wt.%), Al₂O₃ (20.6 –
30 43.9 wt.%), and Fe₂O₃ (9.7 – 22.4 wt.%). The amount of CaO in Meknes clays ranges from 8 to 12 wt.%,
31 whereas CaO is only present in some Tetouan clay (TE4, TE7, TN4 and TN5). A significant densification
32 of ceramic behaviour could be noticed for most of Tetouan clays at firing temperatures above 1000°C.
33 Meknes clays show earlier densification from 800 °C. The chemical, textural and ceramic properties of
34 Tetouan and Meknes clays indicate their suitability as raw materials for the production of structural
35 ceramics. The high amount of Fe₂O₃ in all clays makes them inappropriate in fine ceramics.
36

37 **KEYWORDS:** Clay materials, Ceramic properties, Ceramic suitability, Morocco.
38
39
40
41
42
43
44
45
46
47
48
49

50 1. Introduction

51 Throughout the world, clays are the main raw materials exploited in the fabrication of various ceramic
52 products for building construction. Due to inherently complex physical, chemical and mineralogical
53 characteristics, clays have unique properties related to their own natural genesis [1-4]. In most cases, for
54 economic reasons, the ceramics industry relies on clays from nearby deposits. As a consequence, the
55 characterization and quality control of each clay is important for the technical performance of local
56 products [5, 6].

57 Pure clays do not occur in nature, they contain mixtures of different clay and associated minerals [7-9]. At
58 present, many ceramic tiles are manufactured from mixtures of mineral raw materials, composed
59 essentially of clays and materials such as quartz, feldspar and carbonates. In the fabrication process, the
60 raw materials are mixed in variable proportions taking into account the influence of each component on
61 the properties of the final products [10, 11]. The components that play fundamental roles for optimum
62 processing, and hence performance of the final products, are clay fraction ($< 2\mu\text{m}$) for plasticity, feldspar
63 for fluxing and silica as filler material [12-14]. The selection of the appropriate raw materials is based on
64 specific criteria, which are related either to the behaviour during the different stages of manufacturing or
65 to the overall chemical composition. The microstructure and properties of any ceramic depends on the
66 characteristics of the raw materials and processing parameters [15] to assure the quality of ceramic
67 products.

68 Morocco is among the world top 20 producers and consumers of clayey building materials
69 (<http://www.lematin.ma/reader-2007/files/lematin/2011/01/30>). The industry of ceramic tiles and bricks is
70 most frequent in northern Morocco. Natural clayey materials are abundant in this region. They play an
71 important economic role with a national production of about 45% for building materials (bricks, ceramic
72 tiles and refractories). However, national ceramic production is still insufficient, and to fill this deficit the
73 Moroccan government has to import ceramic products mainly from Spain, Italy and Egypt.

74 The Tetouan and Meknes area have large construction and development projects to meet the population
75 growth in particular for social and luxury housing construction, which is experiencing a significant
76 economic and tourism development. Meknes and Tetouan clays are currently used for the traditional
77 production of small-scale ceramic factories. Meknes clays are used in small traditional pottery factories
78 using local clays. Artisanal and semi-industrial exploitation of these clays, without any prior study, causes
79 various problems during the manufacturing process, such as deformations and breakage of products.

80 The aim of this study is to evaluate the viability of the Tetouan and Meknes clay deposits as an industrial
81 mineral resource by comparing their textural, chemical and thermal properties as well as drying and firing
82 behaviours.

84 2. Material

85 The studied clayey raw materials were collected in the Tetouan and Meknes areas. The Tetouan clay
86 deposit is located in north-western Morocco a few kilometres from the town of Tetouan, in the external
87 Rif domain [17] (Fig. 1). A total of nineteen clay samples were collected in this area. There are two
88 categories of samples: 10 clay samples collected from the exploited quarries labelled (TE) and 9 clays
89 sampled from clay deposits, which are not yet exploited, labelled (TN). The Meknes clay deposit is
90 located in north-central Morocco, about 15 km east of the town of Meknes, in the Saïss Basin zone
91 situated in the Pre-Rif domain (Fig. 1). Six Miocene yellow sandy clay samples [18] were collected from
92 the quarries of pottery and artisanal ceramic.

93 A preliminary characterization of those clay materials was done in a previous study [19]. Tetouan clays
94 are characterized by diversified mineralogical assemblages (in particular a variable proportion of clay,
95 quartz and calcite) in contrast with to Meknes clays (high clay content, quartz and calcite). The clay
96 fraction of Tetouan is dominated by illite and kaolinite with variable contributions of chlorite. Meknes
97 clays are illite and kaolinite, associated with smectite. The studied clay materials consist generally of fine
98 particles with medium to high plasticity and low organic matter content [19].

100 3. Analytical methods

101 3.1. Textural properties

102 The specific surface area of the samples was characterized by the analysis of nitrogen adsorption–
103 desorption isotherms, performed at 77 °K. The measurements were performed using a sorptomatic Carlo
104 Erba 1900, controlled by a computer (Industrial Chemistry, Department of Chemistry, ULg). The analysis

105 of the isotherms was performed according to the methodology of Vallée, Keller [20], which provided
106 specific surface area (S_{BET}), micropore volume calculated by the Dubinin–Radushkevich equation
107 (VDUB), and total pore volume calculated from the adsorbed volume at saturation (V_p). The bulk density
108 (ρ_s) was obtained by helium pycnometry on the powdered sample, using Micromeritics Accucyc 1330.
109 Textural analyses were done at the laboratory of Industrial Chemistry (Department of Chemistry, ULg).
110 Cation Exchange Capacity (CEC) was measured by the Schollenberger method [21]. The samples were
111 first saturated by ammonium acetate (1N), and then the ammonium ions in the supernatant were
112 deprotonated into ammonia with sodium hydroxide solution (0.1N). The ammonia content was then
113 determined by distillation into a known amount of acid and back-titrated by the Kjeldahl method [22].
114

115 3.2. Chemical and thermal properties

116 The chemical composition of selected elements (Si, Al, Fe, Ca, Mn, Mg, Na, K, Ti, P and S) was
117 measured as oxides on 2 g of dried and homogenized powder of clayey samples using a Bruker S8 Tiger
118 wavelength-dispersive X-Ray Fluorescence (WD-XRF) spectrometer equipped with a Rh anticathode
119 (Department of Ecology and Environmental Sciences, Umeå University). Calibration was made using 35
120 commercially available certified reference materials of similar matrix (sedimentary rocks, river, lake and
121 marine sediments, sands and soils). The accuracy ranges from 3 to 7% except for S (25%) and P (20%).
122 Reproducibilities are above 99% except for S (89%) and P (97%). More details about the method and the
123 calibration can be found in [23]. The same powdered samples were heated to 1000 °C for 2h to determine
124 the Loss On Ignition (L.O.I).

125 Differential scanning calorimetry (DSC) and thermogravimetry (TG) were conducted simultaneously
126 using a NETZSCH STA 409 PC instrument (Industrial Chemistry, Department of Chemistry, ULg).
127 Samples were heated from room temperature to 800 °C at 10 °C min⁻¹ under atmospheric air [24].
128

129 3.3. Ceramic properties

130 Industrial tests were carried out as part of the ceramic evaluation process. Clay samples were dried at
131 105°C for 24 hr and ground to a fine powder and then sieved using a mesh-size of 100 μm . Each clay
132 sample was wetted in order to achieve the proper plasticity for modeling. The samples obtained with these
133 shaping techniques were 4 cm long, 2 cm wide and 2 cm thick. The drying was done in a shaded and
134 ventilated room. For different drying times, the mass and the value of the length were measured to
135 calculate the linear shrinkage. The dried samples (24 h at shaded room plus 12 h at 105°C in oven) were
136 kiln-fired at different temperatures (800, 850, 900, 950, 1000, 1050 and 1100°C) over 1 h. The fired
137 samples were tested for loss on ignition, shrinkage and water absorption capacity after firing. The linear
138 shrinkage (LS) was determined following the conventional techniques. The water absorption capacity
139 (WAC) was determined according to standard procedure UNE 67-027 [25], in fired clay pieces after each
140 cooking cycle [26]. After preliminary measurements at the end of firing and cooling, the specimens of
141 each batch were kept dry in an oven until their submission to water absorption. Each dry and cool
142 specimen was weighed (P1) and the three were then immersed into clean water at 25°C for 24 h. The
143 specimens were removed from the water, their surfaces were wiped off and the weight (P2) of each was
144 measured immediately. The water absorption capacity (WAC) was calculated as $\text{WAC} = (\text{P2} - \text{P1})/\text{P1} \times 100\%$.
145
146

147 4. Results and discussion

148 4.1 Textural properties

149 Specific surface area (S_{BET}), pore volume (V_p), micropore volume (VDUB) and cation exchange capacity
150 (CEC) of the samples are listed in Table 1. The surface area of the Meknes samples ranges from 33.3 to
151 37.9 m²g⁻¹. Sample M1 has the highest specific surface area and M3 the lowest. According to these
152 specific surface area values, M1 has less illite and smectite content, knowing that the specific surface area
153 of kaolinite is usually smaller (10-20 m²g⁻¹) with respect to that of illite (80-100 m²g⁻¹) [27], but similar
154 values for smectite (19 m²g⁻¹) [28]. The Tetouan clays have specific surface area (S_{BET}) values ranging
155 between 17 and 36 m²g⁻¹. Among them TE1, TE3 and TN9 display the highest SSA values due to their
156 illite, kaolinite and interstratified clay contents [29].

157 The CEC values of the Meknes samples (9.0-20.6 meq100⁻¹g) are higher than the Teouan clays (7.1-18.5
158 meq100⁻¹g). The high CEC values of the Meknes samples may be explained by their smectite content [19],
159 a mineral characterized by higher CEC value ranging between 80 and 150 meq100⁻¹g [7].
160 The highest S_{BET} and CEC of Meknes and some Tetouan clays (TN and TE) reflect their fine grain size,
161 which is represented by the high amount of clay fraction. The highest S_{BET} and CEC of those clays could
162 cause a difficulty to dry and lead to the development of cracks in the drying process. The bulk density
163 (ρs) of all clay samples are almost similar, ranging from 2.7 to 3.2 gcm⁻³.
164

165 4.2 Chemical and thermal properties

166 The most abundant oxides in the studied samples are SiO₂, Al₂O₃, CaO and Fe₂O₃ (Table 2). According to
167 the major element abundances, the samples are divided into two groups (Fig. 2). The first group is
168 characterized by very low CaO (<1.9%), slightly high Fe₂O₃ (from 12 to 22%) and high Al₂O₃ (from 29
169 to 44%) in comparison to the second group. On the basis of their low CaO content, the first group is
170 qualified as a non-calcareous clay group, which is mainly represented by the Tetouan clays (TE and TN).
171 The second group displays higher CaO (12-22%), slightly lower Al₂O₃ (20-25%) and lower Fe₂O₃ (8-
172 12%) concentrations and is labelled as a moderate calcareous group. Group 2 consists of all the Meknes
173 samples and TE4, TE7 from the exploited Tetouan samples and TN4 and TN5 from unexploited Tetouan
174 clays. The higher contents of Fe₂O₃ (>5%) in the samples give the reddish color of the clay-based
175 products after firing. The L.O.I at 1000°C (Table 2) ranges from 6 to 24%, which is associated with the
176 presence of clay minerals, hydroxides and organic matter [7, 30]. These material losses are confirmed by
177 the thermal analysis and organic matter content as indicated in Fig. 3 and Table 2.
178 The DSC/TG (Fig. 3a and 3b) show at least 4 peaks. The first endothermic peak is observed at 90–150 °C
179 for Tetouan samples and between 96 °C and 113 °C for Meknes samples. Such peaks can be attributed to
180 the removal of adsorbed and interlayered water. The associated mass lost ranges from 0.4 to 0.8% for
181 Meknes clays and between 0.4 and 1.3% for Tetouan clays. A large exothermic peak is observed between
182 200–450°C. Due to organic matter decomposition [31], it was observed in all studied clays, but was
183 especially well marked at 450°C for M6. A broad endothermic band, sintered at 520 to 550°C for Meknes
184 samples and at 523 to 568°C for Tetouan area samples, is due to clay mineral dehydroxylation and α
185 quartz →β quartz transformation [25]. A substantial loss of weight (5–7%) is associated with this
186 endothermic peak for Tetouan samples. As an exception, some Tetouan samples (TN4, TN5, TE7 and
187 TE4) lost less than 3% weight. Meknes samples lost about 4%, demonstrated by elevated clay and quartz
188 content in this area. Small additional endothermic peaks occurred in all samples at 700°C, which are due
189 to carbonate decomposition [32].
190

191 4.3. Ceramic properties

192 a- Drying behaviour

193 Bigot's curves (Fig.4) were used as preliminary indicators in the choice of raw materials [33] for the
194 ceramic industry. The drying is accompanied by shrinkage of the clay materials, due to porewater loss.
195 The Bigot's curves exhibit the two characteristic phases of the drying process: an initial weight loss with
196 shrinkage and successive weight loss with no further shrinkage. The behaviour of all Meknes clay
197 samples was somewhat similar (Fig.4), although there were some small differences in shrinkage, ranging
198 from 12 to 17%, accompanied by a loss of weight from 19 to 22%. Tetouan clay samples showed a low
199 drying shrinkage (2–6%), in contrast to the Meknes clay samples. Tetouan clays showed a greater
200 increase of the loss on weight (20–23%). The highest linear shrinkage of Meknes clays can be explained
201 by its smectite content and its high PI value [34]. Consequently Meknes clays have more problematic
202 drying behaviour. By contrast, Tetouan (TN and TE clays) showed a low drying shrinkage, and they have
203 more suitable behaviour.

204

205 b- Firing behaviour

206 The results for linear firing shrinkage, loss on mass and water absorption of the fired clays are displayed
207 in Table 3 and Fig. 5, respectively. Linear firing shrinkage and water absorption have been frequently
208 used as quality and process control parameters in the development and manufacturing stages of the
209 production of structural ceramics such as floor and wall tiles [35, 36]. The linear firing shrinkage could be

210 used as a direct measure of the extent of densification [37]. The linear firing shrinkage increased
211 gradually from 1000 to 1110°C for most of the Tetouan clays (TN and TE). This evolution reflects
212 densification of the fired clays. As an exception, some fired clays (TE5, TE7 and TE8) do not show any
213 shrinkage. At 800°C, Meknes clays shrank from 17 to 29% and their shrinkage increased again gradually
214 from 850 °C to 1110°C. Meknes clays are characterized by an early densification from 800°C. This is due
215 to the formation of a glassy phase, because they contain large amounts of fluxing agents (Na₂O, K₂O and
216 MgO) (Table 2). Loss on weight stability is indicated from 1000°C for most of the sintered clay bodies
217 (Table 3). It can be seen that an increase in the shrinkage with a decrease in water absorption are
218 associated with an increase in firing temperature. This trend is found especially above 1000°C. Shrinkage
219 is related to the formation of high temperature crystalline phases, and the rates of shrinkage are directly
220 related to the development of glassy material. Formation of gases during vitrification can also have a
221 significant effect on the net dimensions of fired clay minerals. The greatest shrinkage above 1000°C is
222 due to a more significant liquid phase formation. During liquid phase formation, the liquid surface tension
223 and capillarity help to bring particles close together and reduce porosity [38].

224 A significant decrease of the water absorption is observed for Tetouan clays (TE and TN) from 1000 °C
225 (Fig. 5). As an exception, TE4 and TN4 present the highest water absorption capacity (about 18%). The
226 Meknes clays have high water absorption capacity, ranging from 9 to 21%. At 1100 °C, the water
227 absorption of Tetouan clays decreased to 0.4% and 2.6% for TE6 and TN8, respectively, indicating the
228 total vitrification of those clays. For Meknes clays, the water absorption decreased from 6 to 13%, with
229 the exception of M1, which had 20 % (Fig. 5).

230

231 4.4. Suitability for ceramics applications

232 The suitability of raw clay for their use in the manufacture of ceramic products is determined by
233 mineralogy, chemistry and physical properties of the material. These factors will determine the behaviour
234 of the clay during forming, drying and firing with direct influence on the final product [39]. In order to
235 evaluate the suitability of the studied clays for different ceramic products, a ternary diagram from [40]
236 based on XRD results [19] is shown in figure 6a. Two groups can be identified: those with high quartz
237 contents and those that are rich in oxides, carbonates and feldspars. The mineralogical data for the
238 samples (Fig. 6b) also suggest that most of the Meknes clays can be used for vitrified red floor tile
239 making. However Tetouan clays can be used for different ceramic applications due to their high quartz
240 amount and their low amount of iron oxide. TN7 and TE9 may be used for making clinker products and
241 TE7 for vitrified red floor tiles (Fig. 6c). Some Tetouan samples (TN5, TN9 and TE7) are located close to
242 the porous light-coloured field; they can therefore be used for porous light-coloured wall tile product.

243 The ternary diagram (Fe₂O₃ + CaO + MgO)/Al₂O₃/(Na₂O + K₂O) (Fig. 6c) is used to classify raw clay
244 materials and industrial ceramic bodies [40]. All Meknes clays plot in the field of red ceramics, close to
245 the field for porous light-coloured ceramics. Most of the Tetouan clays were located outside of the red
246 ceramics field, with the exception of TE4, TE7, TN4 and TN5, which are close to the field for porous
247 light-coloured ceramics. The ideal composition for an optimum white body product (SiO₂ = 72 wt%,
248 Al₂O₃ and total oxides = 8 wt%) was estimated by Fiori *et al.*, [40], Wilson [41] and Baccour *et al.*, [42],
249 who stated that clays containing 8% or more of Fe₂O₃ are red-firing clays. In this context, none of the
250 Meknes and Tetouan clays can be used for the production of fine ceramics, due to their high Fe₂O₃
251 amount (> 8%). Such application would require processing to reduce this iron oxide content. However,
252 Tetouan clays could be considered as raw materials for structural ceramic products.

253 The high firing shrinkage for M1 and M3 from Meknes area (>10%) make them inappropriate to make
254 ceramics, due to the risk of dimensional defects. Water absorption can restrict the use of ceramics as
255 building material [37, 43]. Ceramics used as flooring should have a water absorption < 1%, roofing tiles <
256 20%. Some Tetouan (TE1, TE2, TE3, TE6, TE9 and TN8) clays can also be used as flooring. Meknes
257 clays and most of unexploited Tetouan clays show adequate water absorption for a use as roofing tiles.
258

259 5. Conclusion

260 Tetouan and Meknes clay materials are composed mainly of SiO₂, Al₂O₃, and Fe₂O₃. Meknes clays are
261 characterized by a higher CaO content.

262 The ceramic behaviours of Tetouan and Meknes clays were interpreted by drying shrinkage, linear firing
263 shrinkage, loss on weight and water absorption. Meknes clays are characterized by a high drying
264 shrinkage, and therefore there will be more difficulty to dry the samples. To solve this problem, sand
265 could be added to reduce their plasticity. Tetouan clays show optimal drying shrinkage. All the fired
266 ceramic properties show moderate changes from 800 to 1000°C. However, significant changes are
267 observed above 1000 °C. An increase in the firing shrinkage and associated with a decrease in the water
268 absorption are especially observed from 1100°C.
269 Meknes clays and most of Tetouan clays (TE1, TE2, TE3, TE6, TE9 and TN8) can be used on flooring
270 production. In addition some exploited Tetouan clays and currently unexploited Tetouan clays are also
271 suitable for making roofing tiles. Meknes clays and most of the Tetouan clays can be used for different
272 ceramic applications due to their high quartz amount and their small iron oxide amount. Only TN7 and
273 TE9 are being used for making clinker products.
274 This study demonstrates that exploited Tetouan and Meknes raw clay are suitable for the manufacture of
275 structural ceramic products, with or without additives depending on the ceramic type. New clay outcrops
276 such as unexploited Tetouan clays are also suitable. They constitute a potential ceramic raw material for
277 growing Moroccan ceramic tile industry, and are thus not limited to artisanal production.

278 **Acknowledgements**

279 The WD-XRF data acquisition was made possible at Umeå University through a research grant from the
280 Kempe Foundation to Richard Bindler. The authors would like to thank René Pirard (Laboratoire de
281 Génie Chimique, Université de Liège, Belgium) for the Calorimetry (ATD-TG) and specific surface area
282 (SSA) analyses. We would like to thank Anne Iserentant (Université catholique de Louvain) for the CEC
283 analysis. Finally, our thanks go to Dekayir (Université de Marrakech, Morocco) for his help on the field.

284 **References**

- 285
- 286
- 287 [1] B. Bauluz, M.J. Mayayo, C. Fernández-Nieto, G. Cultrone, J.M. González López, "Assessment of
288 technological properties of calcareous and non-calcareous clays used for the brick-making industry of
289 Zaragoza (Spain)", *Applied Clay Science*, 2003, Vol. 24, N°. 1-2, pp. 121-126.
- 290 [2] C. Gomes, "Argilas. O que são e para que servem", Fundação Calouste Gulbenkian, Lisboa, 1989.
- 291 [3] M. Hajjaji, S. Kacim, M. Boulmane, "Mineralogy and firing characteristics of a clay from the valley
292 of Ourika (Morocco) ", *Applied Clay Science*, 2002, Vol. 21, N°. 3-4, pp. 203-212.
- 293 [4] A.G. Verduch, "Características de las Arcillas Empleadas en la Fabricación de Ladrillos", *Técnica
294 Cerámica*, 1995, Vol. 232, pp. 214–228.
- 295 [5] B. Fabbri, "Quality assurance of ceramic clays - a deeper understanding", Schmid, Freiburg,
296 Allemagne, 1994.
- 297 [6] E. Sánchez, F. Ginés, J. Agramunt, M. Monzó, "Control de calidad de las arcillas empleadas en la
298 fabricación de los soportes de baldosas cerámicas". In: *Proceedings Qualicer 98*. Castellón, España, 1998,
299 pp 97–112.
- 300 [7] R.E. Grim, "Clay Mineralogy", McGraw-Hill, New York, 1968.

- 301 [8] D.M. Moore, R.C. Reynolds, "X-ray Diffraction and the Identification and Analysis of Clay
302 Minerals", Oxford Univ. Press, Oxford, New York, 1997.
- 303 [9] F. Bergaya, G. Lagaly, Chapter 1 "General Introduction: Clays, Clay Minerals, and Clay Science", in:
304 B.K.G.T. Faïza Bergaya, L. Gerhard (Eds.), "Developments in Clay Science", Elsevier 1, 2006, pp 1-18
- 305 [10] S.J.G. Sousa, J.N.F. Holanda, "Development of red wall tiles by the dry process using Brazilian raw
306 materials", *Ceramics International*, 2005, Vol. 31, N°. 2, pp. 215-222.
- 307 [11] S. Sousa, J. Holanda, "Thermal transformations of red wall tile pastes", *Journal of Thermal Analysis
308 and Calorimetry*, 2007, Vol. 87, N°. 2, pp. 423-428.
- 309 [12] E. Kamseu, C. Leonelli, D.N. Boccaccini, P. Veronesi, P. Miselli, G. Pellacani, U.C. Melo,
310 "Characterisation of porcelain compositions using two china clays from Cameroon", *Ceramics
311 International*, 2007, Vol. 33, N°. 5, pp. 851-857.
- 312 [13] A.C.S. Alcântara, M.S.S. Beltrão, H.A. Oliveira, I.F. Gimenez, L.S. Barreto, "Characterization of
313 ceramic tiles prepared from two clays from Sergipe - Brazil", *Applied Clay Science*, 2008, Vol. 39, N°. 3-
314 4, pp. 160-165.
- 315 [14] H. Celik, "Technological characterization and industrial application of two Turkish clays for the
316 ceramic industry", *Applied Clay Science*, 2010, Vol. 50, N°.2, pp. 245-254.

- 317 [15] W. Kingery, H. Bowen, D. Uhlmann, "Introduction to Ceramics", New York, John Wiley & Sons,
318 1976.
- 319 [16] M. Durand Delga, L. Hottinger, J. Marcáís, M. Mattauer, Y. Lilliard, G. Suter, "Livre à la mémoire
320 du Professeur Paul Fallot consacré à l'évolution paléogéographique et structurale des domaines
321 méditerranéens et alpins d'Europe", Société géologique de France 1, 1960-1962, pp 399-422.
- 322 [17] W. Wildi, "La chaîne tello-rifaine (Algérie, Maroc, Tunisie): structure, stratigraphie et évolution du
323 Trias au Miocène", Rev. Géol. dyn. Géogr. Phys, 1983, Vol. 24/3, pp. 201-297.
- 324 [18] L. Aït Brahim, "Tectonique cassante et états de contraintes récentes au nord du Maroc", Thèse de
325 doctorat de l'Université Mohamed, 1991, pp. 360.
- 326 [19] M. El Ouahabi, L. Daoudi, N. Fagel, Preliminary mineralogical and geotechnical characterization of
327 clays from Morocco: application to ceramic industry, Clay Minerals, 2014, Vol. 49, pp.1-17.
- 328 [20] A.J. Lecloux, "Texture of catalysts" In: J.R. Anderson and M. Boudart, Editors, Catalysis, science
329 and technology, Springer, Berlin, 1981, Vol.2, pp. 171–230.
- 330 [21] C.J. Schollenberger, R.H. Simon, "Determination of exchange capacity and exchangeable bases in
331 soil. Ammonium acetate method", Soil Science, 1945, Vol. 59, pp. 13–24.

- 332 [22] R.C. Mackenzie, "A micromethod for determination of cation exchange capacity of clay", Clay
333 Minerals (Bull.), 1952, pp. 203-204.
- 334 [23] F.d. Vleeschouwer, V. Renson, P. Claeys, K. Nys, R. Bindler, "Quantitative WD- XRF calibration
335 for small ceramic samples and their source material", Geoarchaeology, 2011, Vol. 26, N°. 3, pp. 440-450.
- 336 [24] M. Abajo, "Manual sobre Fabricación de Baldosas", Tejas y Ladrillos Ed. Beralmar S. A, Barcelona,
337 2000.
- 338 [25] U. 67-027-84, "Determinacion de la absorcion de agua de ladrillos de arcilla", Instituto Espanol de
339 Normalizacion, AENOR, 1984.
- 340 [26] I. 10545-3, "International Standard for Ceramic tiles - Part 3", Determination of water absorption,
341 apparent porosity, apparent relative density and bulk density, International Organization for
342 Standardization, 1995.
- 343 [27] S. Ferrari, A.F. Gualtieri, "The use of illitic clays in the production of stoneware tile ceramics",
344 Applied Clay Science, 2006, Vol. 32, N°. 1-2, pp.73-81.
- 345 [28] J.a.S. Ravichandran, B., "Properties and catalytic activity of acid-modified montmorillonite and
346 vermiculite", Clays Clay Miner, 1997, Vol. 45, pp. 854-858.

- 347 [29] O. Omotoso, R.J. Mikula, P.W. Stephens, "Surface area of interstratified phyllosilicates in athabasca
348 oil sands from synchrotron XRD", *Advances in X-ray Analysis*, 2002, Vol. 45, pp. 363–391.
- 349 [30] F.A.C. Milheiro, M.N. Freire, A.G.P. Silva, J.N.F. Holanda, "Densification behaviour of a red firing
350 Brazilian kaolinitic clay", *Ceramics International*, 2005, Vol. 31, N°. 5, pp. 757-763.
- 351 [31] H. Baccour, M. Medhioub, F. Jamoussi, T. Mhiri, "Influence of firing temperature on the ceramic
352 properties of Triassic clays from Tunisia", *Journal of Materials Processing Technology*, 2009, Vol. 209,
353 N°. 6, pp. 2812-2817.
- 354 [32] S. Yariv, "The role of charcoal on DTA curves of organo-clay complexes: an overview", *Applied
355 Clay Science*, 2004, Vol. 24, N°. 3-4, 225-236.
- 356 [33] I. Štubn̂a, F. Chmelík, A. Trník, P. Šín, "Acoustic emission study of quartz porcelain during heating
357 up to 1500°C", *Ceramics International*, 2012, Vol. 38, N°. 8, pp. 6919-6922.
- 358 [34] S. Maitra, A. Choudhury, H. Das, M. "Pramanik, Effect of compaction on the kinetics of thermal
359 decomposition of dolomite under non-isothermal condition", *Journal of Materials Science*, 2005, Vol. 40,
360 N°. 18, pp. 4749-4751.
- 361 [35] M. Dondi, B. Fabbri, G. Guarini, "Grain-size distribution of Italian raw materials for building clay
362 products: a reappraisal of the Winkler diagram", *Clay Minerals*, 1998, Vol. 33, N°. 3, pp. 435-442.
- 363

- 364 [36] D.A.C. Manning, "Introduction to industrial minerals", 1st ed., Chapman & Hall, London ,1995.
- 365 [37] S.L. Correia, K.A.S. Curto, D. Hotza, A.M. Segadães, "Using statistical techniques to model the
366 flexural strength of dried triaxial ceramic bodies", Journal of the European Ceramic Society, 2004, Vol.
367 24, N°. 9, pp. 2813-2818.
- 368 [38] S.L. Correia, D. Hotza, A.M. Segadães, "Simultaneous optimization of linear firing shrinkage and
369 water absorption of triaxial ceramic bodies using experiments design", Ceramics International, 2004, Vol.
370 30, N°. 6, pp. 917-922.
- 371 [39] F.P. Shepard, Nomenclature based on sand-silt-clay ratios, Journal of Sedimentary Petrology, 1954,
372 Vol. 24, pp. 151-158.
- 373 [40] S.N. Monteiro, C.M.F. Vieira, "Influence of firing temperature on the ceramic properties of clays
374 from Campos dos Goytacazes", Brazil, Applied Clay Science, 2004, Vol. 27, N°. 3-4, pp. 229-234.
- 375 [41] C.C. Mardare, A.I. Mardare, J.R.F. Fernandes, E. Joanni, S.C.A. Pina, M.H.V. Fernandes, R.N.
376 Correia, "Deposition of bioactive glass-ceramic thin-films by RF magnetron sputtering", Journal of the
377 European Ceramic Society, 2003, Vol. 23, N°. 7, pp. 1027-1030.
- 378 [42] C. Fiori, B. Fabbri, G. Donati, I. Venturi, "Mineralogical composition of the clay bodies used in the
379 Italian tile industry", Applied Clay Science, 1989, Vol. 4, N° 5-6, pp. 461-473.

- 380 [43] H.H. Murray, "Applied clay mineralogy", Developments in Clay Science 2Elsevie B.V, 2007.
- 381 [44] A.T. Machado, F.R. Valenzuela-Diaz, C.A.C. de Souza, L.R.P. de Andrade Lima, "Structural
382 ceramics made with clay and steel dust pollutants", Applied Clay Science, 2011, Vol. 51, N°. 4, pp. 503-
383 506.
- 384 [45] M. Saadi, E.A. Hilali, A. Boudda, "Carte Géologique de la chaîne Rifaine - échelle 1:500.000",
385 Ministère de l'Energie et des Mines, Direction de Géologie, Service de Géologie du Maroc. Notes et
386 Mémoires, 1980, N° 245.

387

388

389 **Tables**

390 Table 1. Textural properties of the clay samples.

391 S_{BET} : specific surface area; V_p : pore volume; $VDUB$: micropore volume; CEC : specific surface area; ρ_s :
392 bulk density.

Samples	S_{BET} ($m^2 g^{-1}$)	V_p ($cm^3 g^{-1}$)	$VDUB$ ($cm^3 g^{-1}$)	CEC ($meq 100^{-1} g$)	ρ_s ($g cm^{-3}$)
	± 5	± 0.05	± 0.01		
Meknes					
M1	37.9	0.055	0.015	12.9	2.7
M2	36.3	0.055	0.015	9.1	2.7
M3	33.3	0.053	0.015	9.7	2.7
M4	36.3	0.053	0.015	10.1	2.7
M5	34.7	0.049	0.015	20.6	2.7
M6	35.2	0.094	0.015	12.5	2.7
Unexploitable Tetouan clays					
TN1	32.4	0.069	0.015	18.5	2.7
TN2	32.9	0.072	0.015	17.1	2.8
TN3	31.0	0.072	0.015	17.2	2.8
TN4	34.6	0.08	0.02	8.5	2.8
TN5	26.2	0.061	0.014	10.0	2.8
TN6	27.9	0.064	0.015	18.3	2.7
TN7	26.2	0.086	0.012	13.1	2.8
TN8	30.2	0.091	0.012	9.3	2.8
TN9	36.4	0.101	0.015	17.9	2.8
Exploitable Tetouan clays					
TE1	35.5	0.077	0.015	13.8	2.8
TE2	34.5	0.075	0.015	14.6	2.8
TE3	36.4	0.078	0.015	10.3	2.8
TE4	31.0	0.068	0.014	10.7	2.9
TE5	26.0	0.069	0.011	7.6	2.9
TE6	17.7	0.047	0.008	12.0	2.8
TE7	18.1	0.048	0.01	7.1	2.8
TE8	21.3	0.056	0.01	13.7	3.0
TE9	18.2	0.048	0.008	18.1	3.2

TE10	27.0	0.062	0.015	17.6	2.8
------	------	-------	-------	------	-----

393

394 Table 2. Chemical composition of the clay samples.

	SiO ₂	Al ₂ O ₃	Fe ₂ O ₃	CaO	MnO	MgO	Na ₂ O	K ₂ O	TiO ₂	P ₂ O ₅	SO ₂	Loss On Ignition
Meknes												
M1	44.9	24.83	14.20	11.38	0.06	2.69	0.81	4.12	0.75	0.28	0.22	17.85
M2	42.7	24.83	12.16	12.67	0.05	2.34	0.78	4.07	0.75	0.25	0.08	17.37
M3	41.3	21.05	15.63	8.15	0.04	2.67	0.84	3.37	0.65	0.24	0.42	18.77
M4	43.1	22.67	13.18	9.95	0.05	2.42	0.84	3.71	0.70	0.24	0.08	17.61
M5	41.0	23.84	14.83	11.70	0.07	1.82	0.67	3.61	0.73	0.22	0.02	18.29
M6	43.1	24.15	12.40	10.47	0.05	2.55	0.92	3.83	0.72	0.26	0.52	16.77
Unexploitable Tetouan clays												
TN1	45.5	30.53	15.84	0.69	0.08	2.06	0.94	3.57	0.90	0.13	0.10	9.90
TN2	47.7	34.58	18.96	0.39	0.03	2.44	0.92	3.49	1.05	0.13	0.00	9.24
TN3	47.1	35.48	22.39	0.25	0.05	2.59	1.16	3.30	1.03	0.14	0.02	8.93
TN4	35.9	20.63	9.75	20.94	0.14	2.14	1.05	3.54	0.53	0.17	0.84	23.90
TN5	35.9	20.90	9.86	22.16	0.15	2.24	1.05	3.52	0.52	0.15	0.68	24.41
TN6	47.6	32.69	14.53	0.48	0.06	1.94	0.86	3.08	0.97	0.12	0.00	8.87
TN7	54.3	30.95	13.38	0.73	0.04	1.94	1.16	2.84	0.90	0.11	0.02	7.48
TN8	51.1	30.46	12.24	1.90	0.03	1.72	1.29	2.89	0.93	0.13	0.10	7.94
TN9	44.2	29.66	15.07	4.55	0.10	1.63	0.89	2.89	1.05	0.27	0.02	11.65
Exploitable Tetouan clays												
TE1	48.6	32.39	17.01	0.45	0.03	1.68	1.78	4.36	0.97	0.18	0.00	7.20
TE2	52.7	31.44	18.01	0.45	0.05	2.36	1.35	2.91	0.83	0.22	0.08	6.82
TE3	54.3	31.48	11.49	0.42	0.03	1.76	1.73	3.95	0.85	0.16	0.02	7.05
TE4	36.7	25.39	9.92	11.84	0.10	6.00	0.94	5.13	0.67	0.10	0.02	19.52
TE5	51.9	33.97	18.10	0.45	0.03	1.89	1.91	4.43	1.00	0.19	0.00	8.72
TE6	51.5	33.78	17.47	0.49	0.03	1.76	1.91	4.41	1.00	0.18	0.06	6.57
TE7	35.0	20.63	8.61	17.67	0.18	5.36	0.81	3.88	0.55	0.11	0.02	21.35
TE8	44.3	43.95	19.87	0.38	0.03	1.19	0.84	6.91	0.78	0.08	0.02	11.13
TE9	48.3	42.40	16.64	0.31	0.02	0.85	1.13	6.07	0.72	0.05	0.02	8.95
TE10	47.6	34.46	20.87	0.41	0.05	2.40	1.11	3.32	1.02	0.14	0.02	8.96

395

396

397

398

399

400

401

402 Table 3. Linear shrinkage (%) of the studied clays during firing process.

	800 °C	850 °C	900 °C	950 °C	1000 °C	1050 °C	1100 °C
Meknes clays							
M1	29.8	23.9	21.7	21.5	21.6	21.4	20.3
M2	19.3	15.3	10.2	9.7	10.2	9.6	8.8
M3	21.8	16.0	14.4	13.9	14.2	14.1	13.8
M4	18.6	13.7	9.3	9.0	9.1	9.0	7.4
M5	18.2	14.2	9.2	8.5	8.8	8.0	7.2
M6	17.4	12.9	9.1	8.8	9.2	8.6	6.7
Unexploitable Tetouan clays							
TN1	0	0	0	0	3.2	3.2	3.2
TN2	0	0	3.1	3.1	3.1	3.1	6.3
TN3	0	0	3.1	3.1	3.1	3.1	3.1
TN4	0	0	2.9	2.9	2.9	2.9	2.9
TN5	0	0	0	0	3.1	3.1	3.1
TN6	0	0	0	0	0	0	3.2
TN7	0	0	0	0	0	3.1	3.1
TN8	0	0	0	0	3.2	3.2	3.2
TN9	0	0	3	3	3	6.1	6.1
Exploitable Tetouan clays							
TE1	0	0	3.1	3.1	3.1	3.1	6.3
TE2	0	0	3.3	3.3	3.3	3.3	3.3
TE3	0	0	3.1	3.1	3.1	3.1	6.3
TE4	0	0	3.3	3.3	3.3	3.3	3.3
TE5	0	0	0	0	0	0	0
TE6	0	0	3.1	3.1	3.1	6.3	6.3
TE7	0	0	0	0	0	0	0
TE8	0	0	0	0	0	0	0
TE9	0	0	0	0	3.1	3.1	6.3

403

404

405

406

407

408

409

410

411

412

413

414

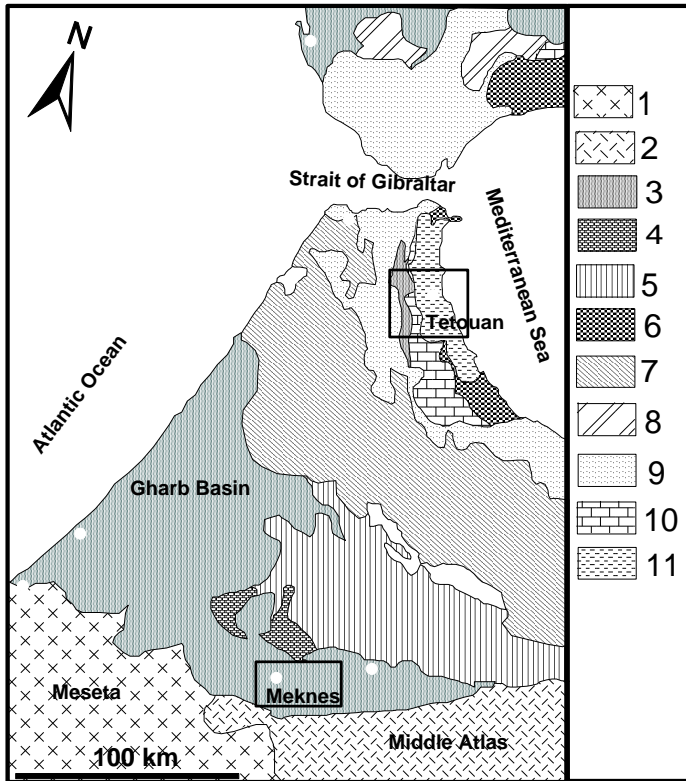
415

416
417
418
419
420
421
422

Figures

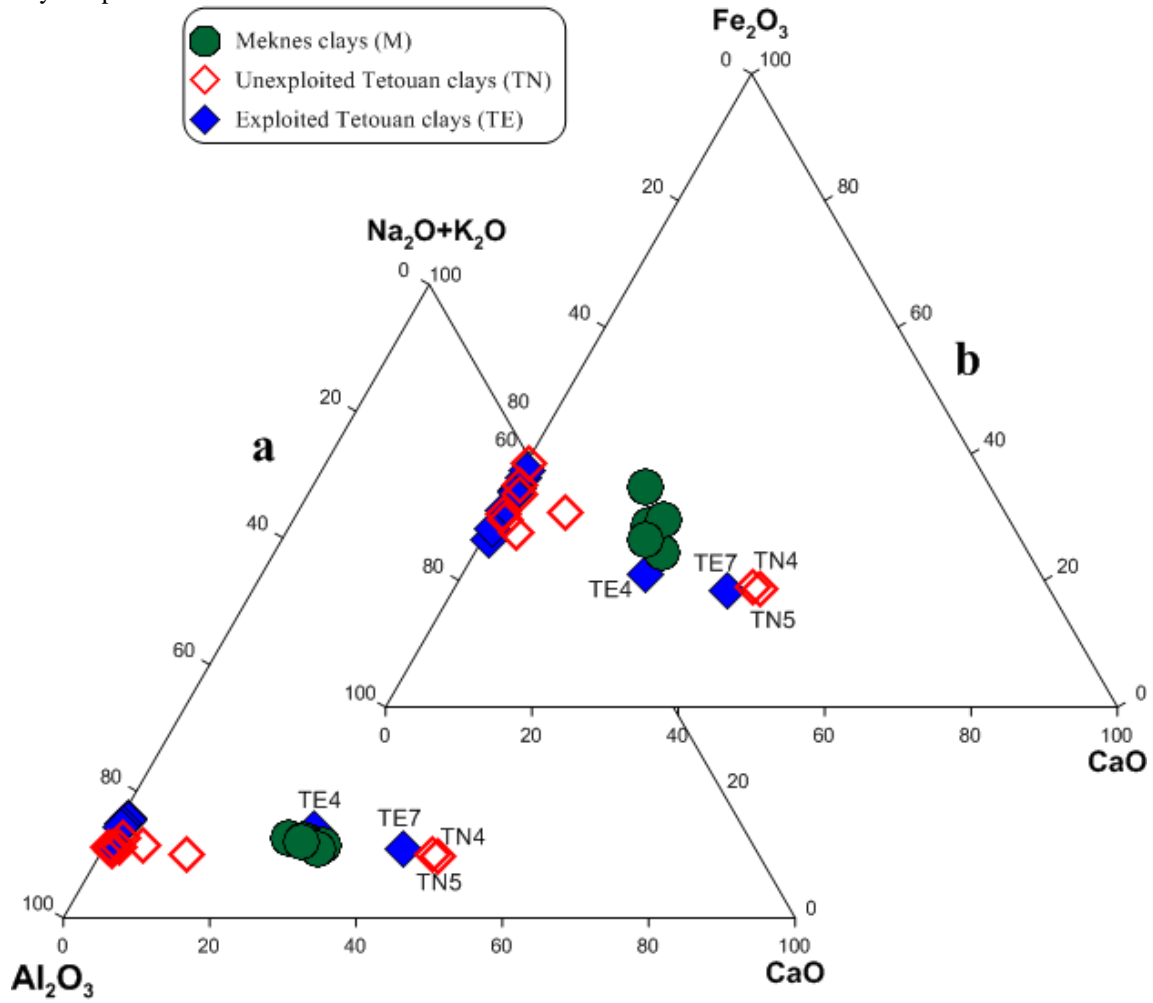
Figure 1. Structural sketch map of the northern occidental part of the Rif Chain and the Northern central of Morocco (modified after [45])

1 – ; Foreland basement, 2 – Meseta and Atlas cover series; 3 – Foredeep basins; 4 – Detached Atlasic cover at Prerif front; 5 – Prerif; 6 – Alpujarrides-Sebtide nappes; 7 –Intrarif, Mesorif, Rif nappes; 8 – Sud-Betic Zone; 9 – Maghrebien Flyschs; 10 – Dorsale calcaire units, 11 –Malaguide-Ghomaride nappes



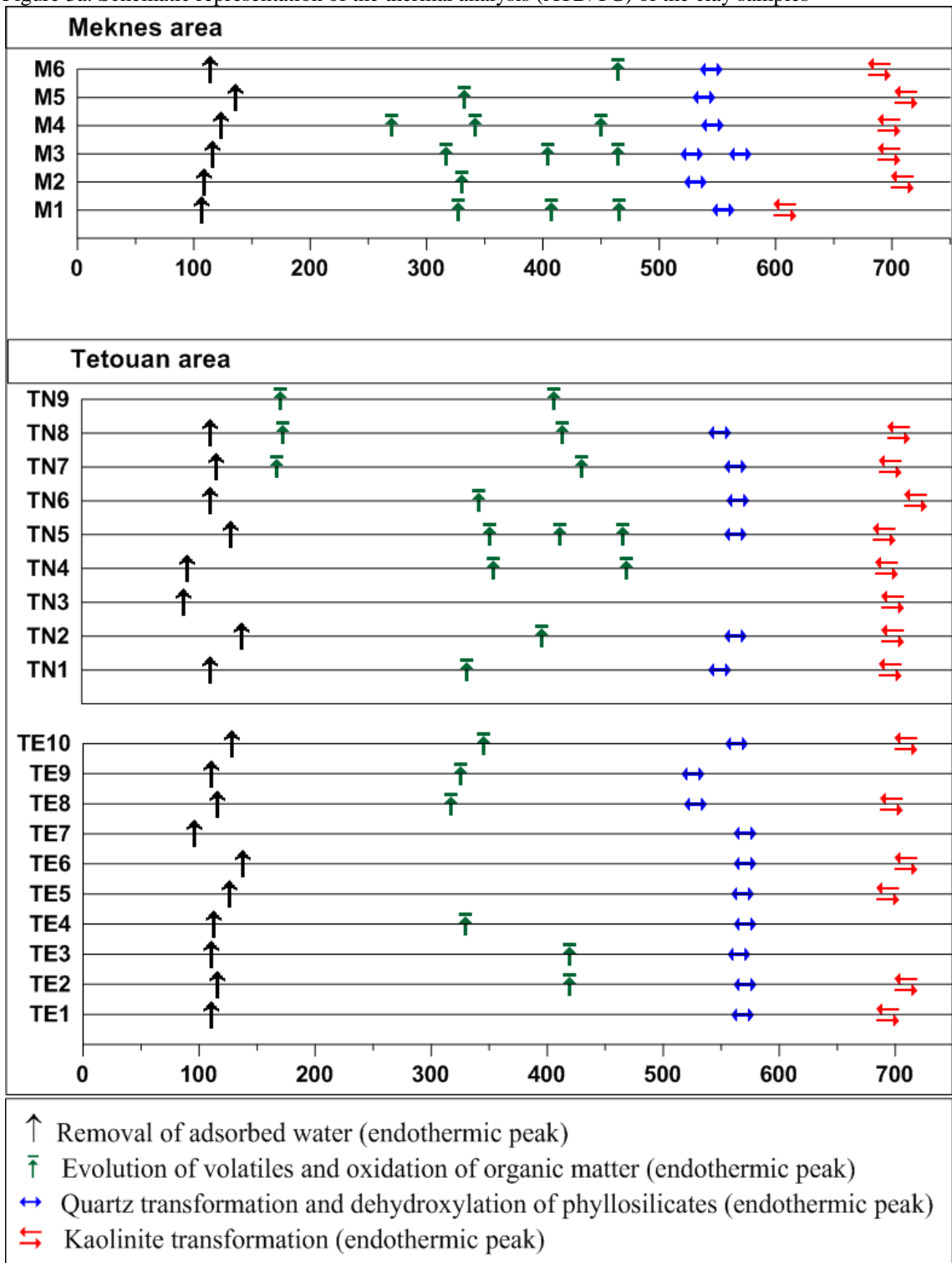
423
424
425
426
427
428
429
430
431
432
433
434
435
436
437
438
439
440
441
442
443
444
445
446
447
448

449 Figure 2. Ternary plot of: (a) Al_2O_3 -CaO- $\text{Na}_2\text{O}+\text{K}_2\text{O}$; and (b) Al_2O_3 -CaO- Fe_2O_3 (all in wt.%) for studied
 450 clay samples



451
 452
 453
 454
 455
 456
 457
 458
 459
 460
 461
 462
 463
 464
 465
 466
 467
 468
 469
 470
 471
 472

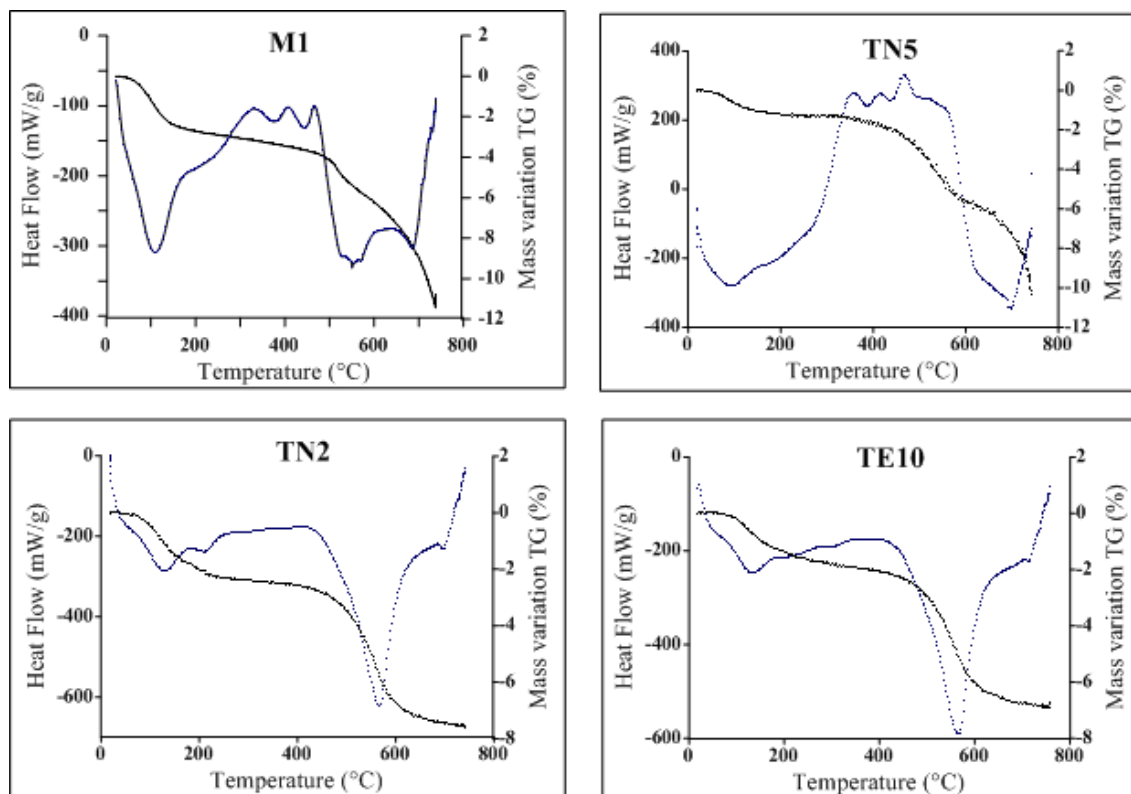
Figure 3a. Schematic representation of the thermal analysis (ATD/TG) of the clay samples



474
475
476
477
478
479
480
481
482

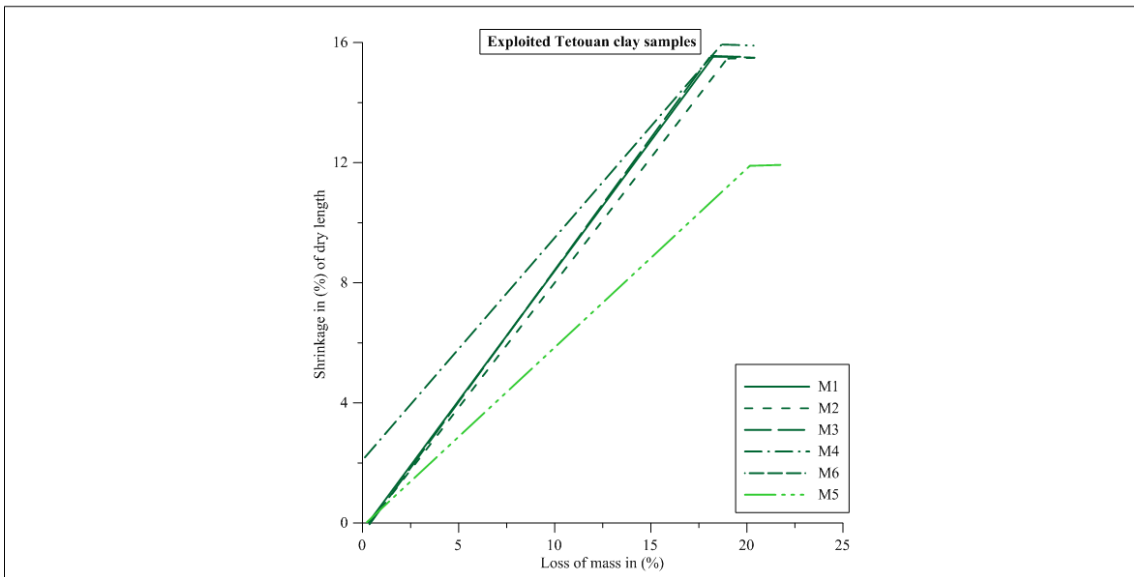
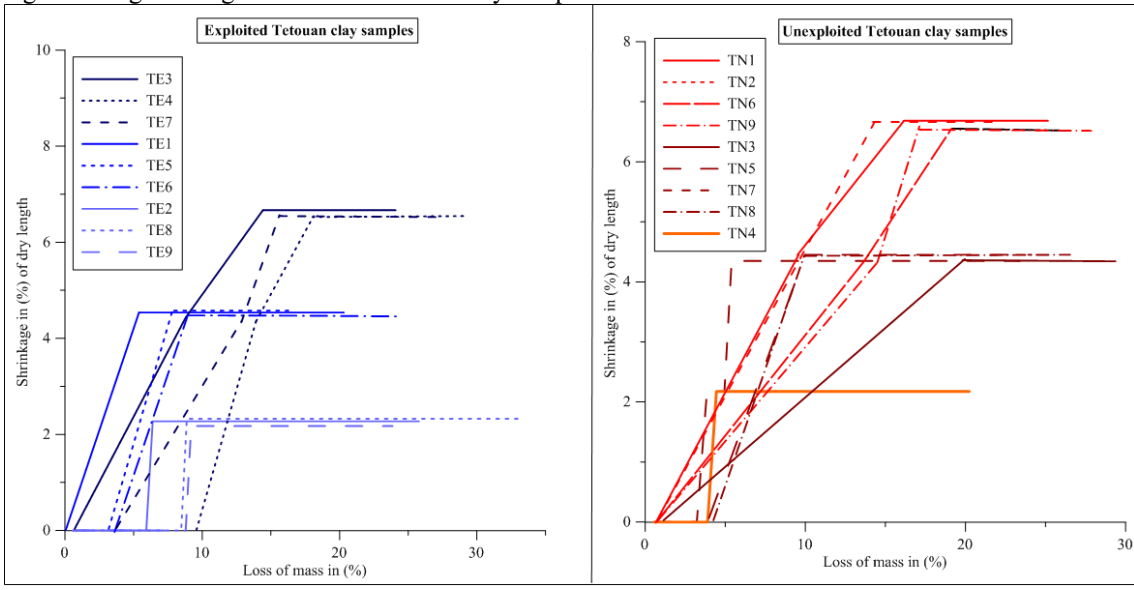
483
484

Figure 3b. Some examples of TG/ DSC curves



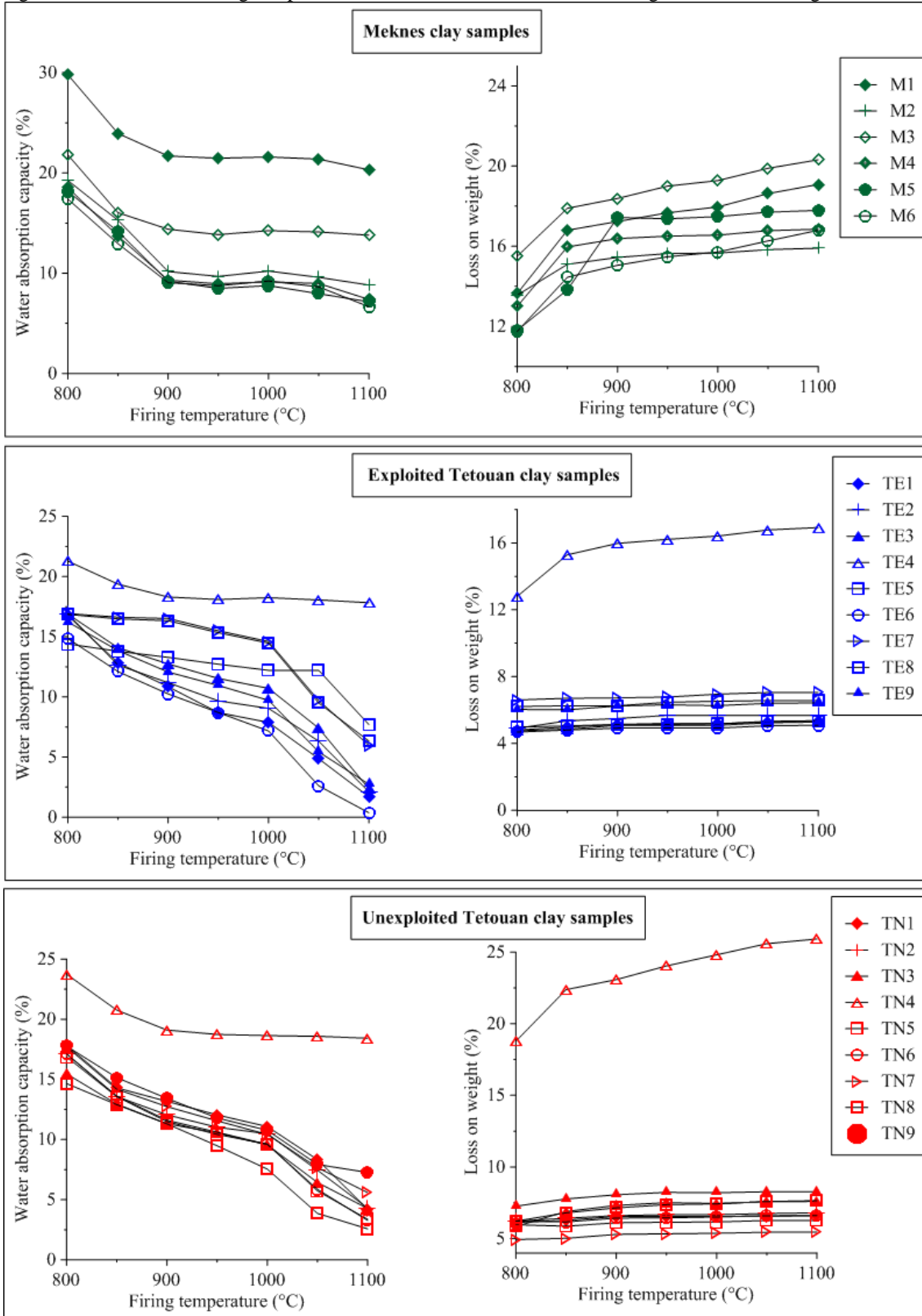
485
486
487
488
489
490
491
492
493
494
495
496
497
498
499
500
501
502
503
504
505
506
507
508
509
510
511
512
513
514

515 Figure 4. Bigot's diagram of the examined clay samples



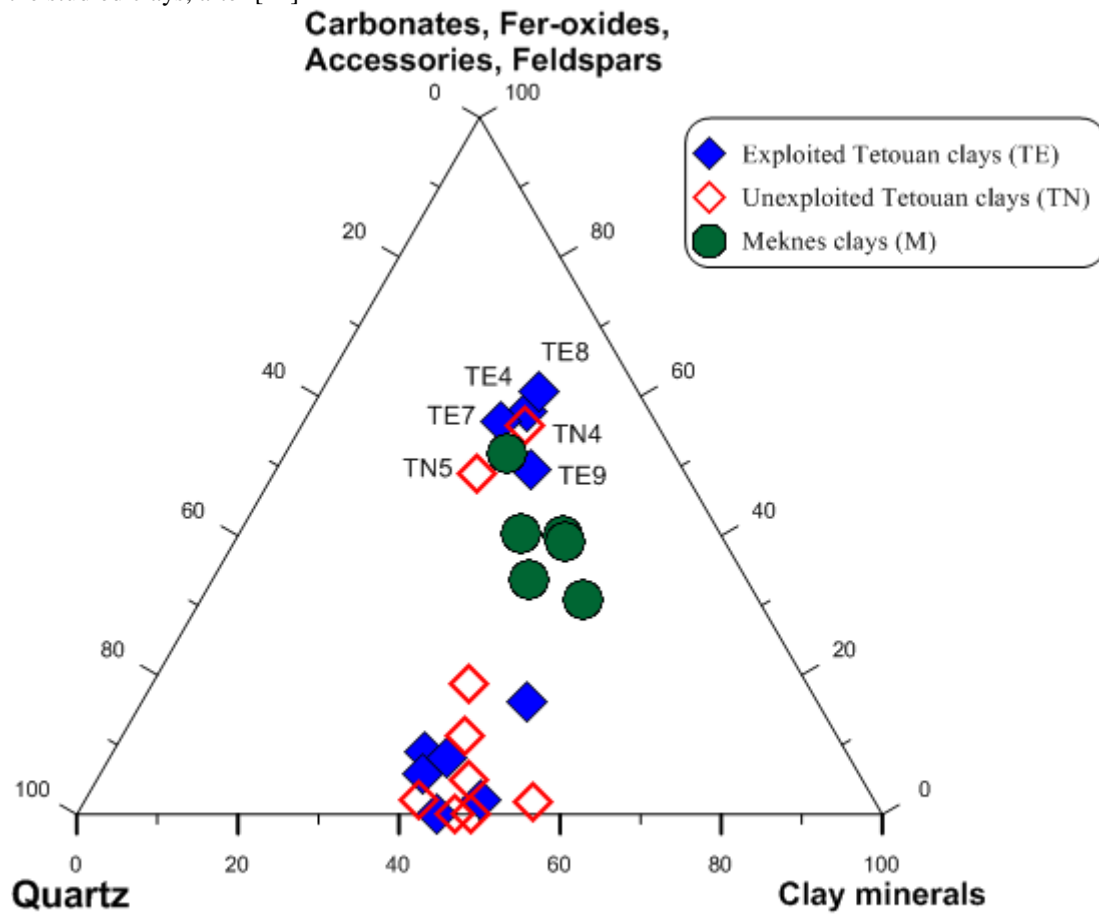
516
 517
 518
 519
 520
 521
 522
 523
 524
 525
 526
 527
 528
 529
 530
 531
 532
 533
 534
 535

Figure 5. Influence of firing temperature on the variation of linear shrinkage and loss on weight



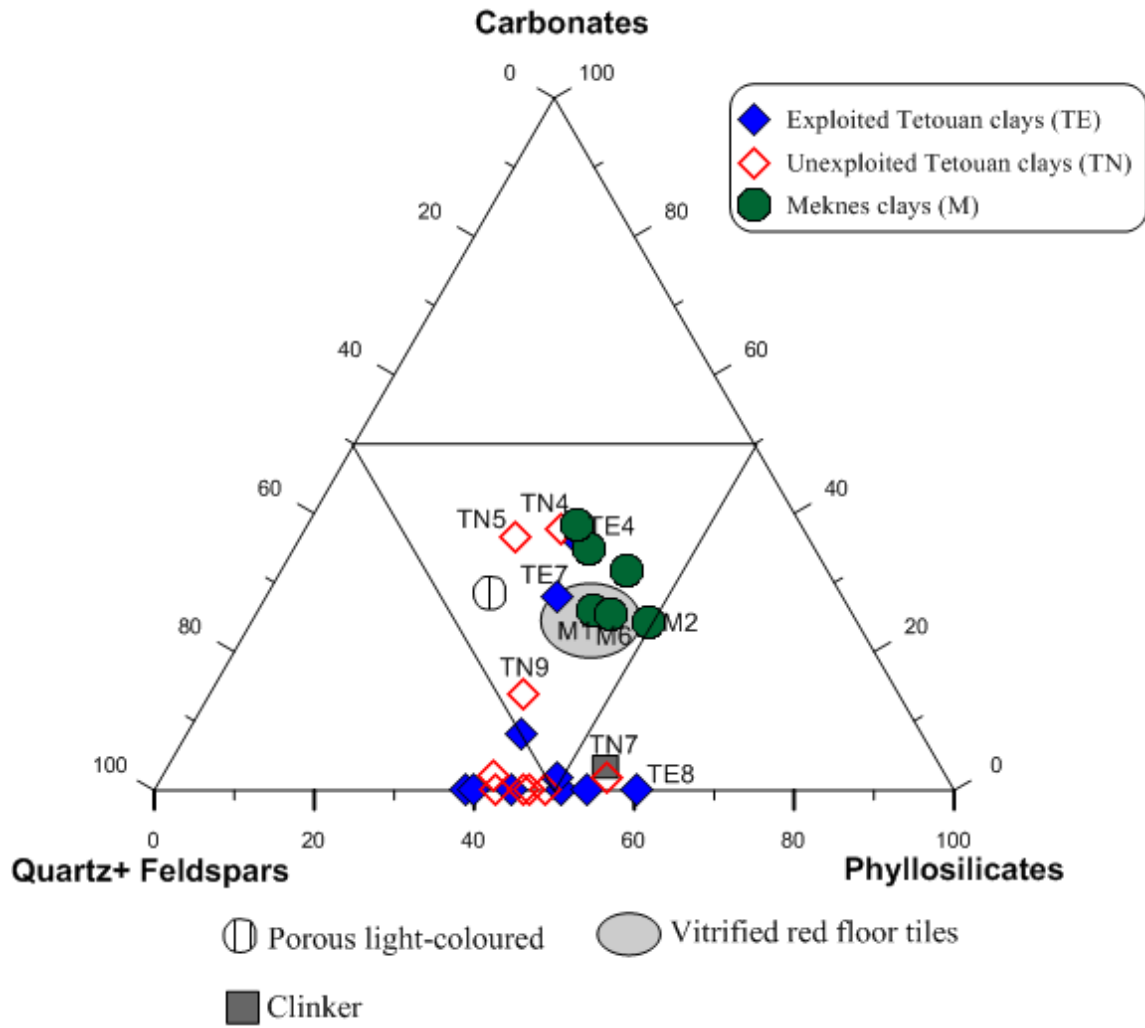
537
538
539
540

541 Figure 6a. Ternary diagram : quartz/ carbonates + Fe-oxides + accessories + feldspars/clays minerals for
 542 the studied clays, after [42]



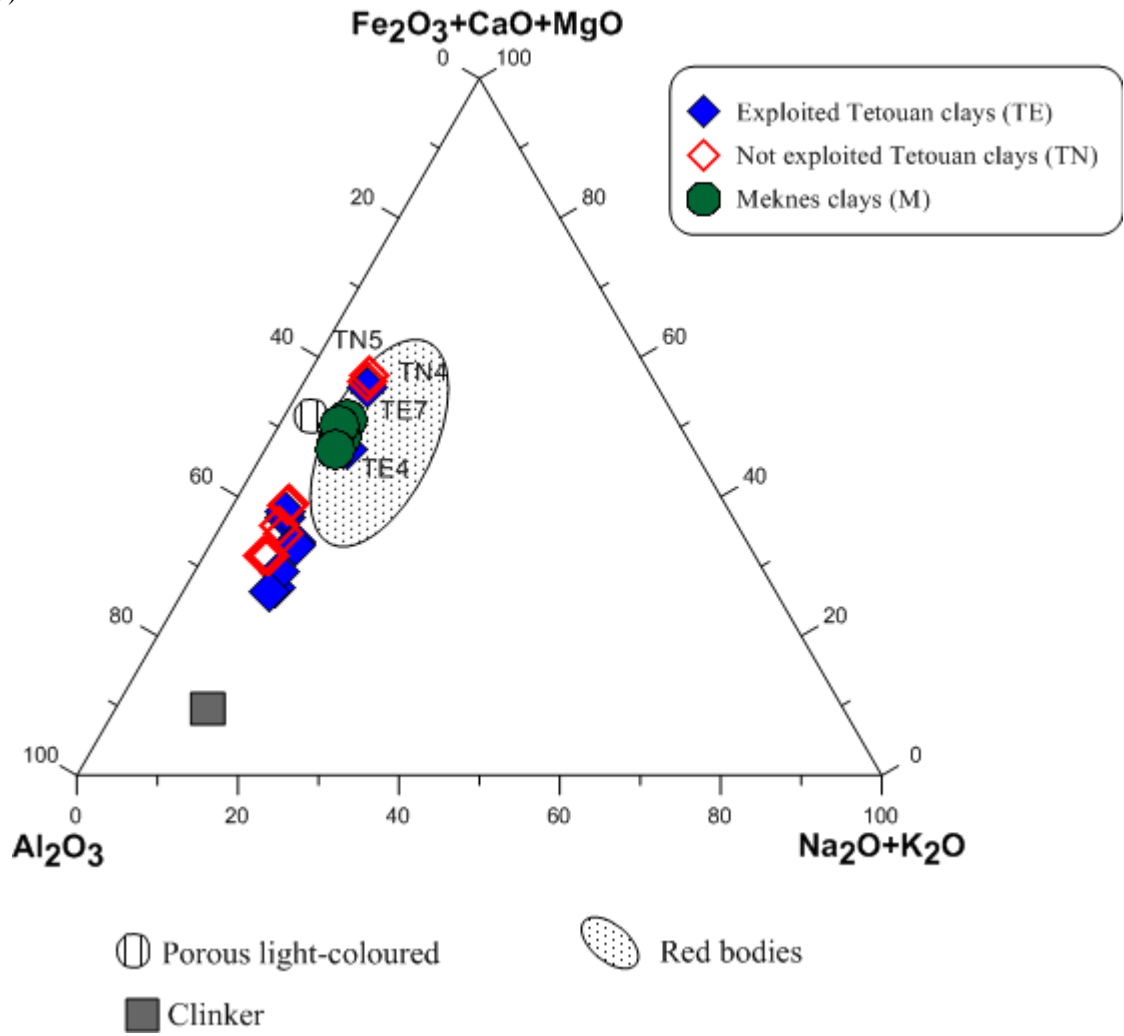
543
 544
 545
 546
 547
 548
 549
 550
 551
 552
 553
 554
 555
 556
 557
 558
 559
 560
 561
 562
 563
 564
 565

566 Figure 6b. Triangular chart : Quartz + feldspars/calcite + dolomite/phyllsilicates for the studied clay
 567 materials, after [42]
 568



569
 570
 571
 572
 573
 574
 575
 576
 577
 578
 579
 580
 581
 582
 583
 584
 585
 586
 587
 588
 589

590 Figure 6c. Ternary diagram of Fiori *et al.*, [42] for clays studied : $\text{Fe}_2\text{O}_3 + \text{CaO} + \text{MgO}/\text{Al}_2\text{O}_3/(\text{Na}_2\text{O} +$
 591 $\text{K}_2\text{O})$



592
 593
 594
 595
 596